Solar Phys (2008) 252: 19–31
DOI 10.1007/s11207-008-9240-6

The Global Solar Magnetic Field Through a Full Sunspot Cycle: Observations and Model Results

Carolus J. Schrijver · Yang Liu

Received: 12 June 2008 / Accepted: 24 June 2008 / Published online: 2 August 2008

Abstract Based on 11 years of SOHO/MDI observations from the cycle minimum in 1997 to the next minimum around 2008, we compare observed and modeled axial dipole moments to better understand the large-scale transport properties of magnetic flux in the solar photosphere. The absolute value of the axial dipole moment in 2008 is less than half that in the corresponding cycle-minimum phase in early 1997, both as measured from synoptic maps and as computed from an assimilation model based only on magnetogram data equatorward of 60° in latitude. This is incompatible with the statistical fluctuations expected from flux-dispersal modeling developed in earlier work at the level of $7-10\,\sigma$. We show how this decreased axial dipole moment can result from an increased strength of the diverging meridional flow near the Equator, which more effectively separates the two hemispheres for dispersing magnetic flux. Based on the combination of this work with earlier long-term simulations of the solar surface field, we conclude that the flux-transport properties across the solar surface have changed from preceding cycles to the most recent one. A plausible candidate for such a change is an increase of the gradient of the meridional-flow pattern near the Equator so that the two hemispheres are more effectively separated. The required profile as a function of latitude is consistent with helioseismic and cross-correlation measurements made over the past decade.

1. Introduction

The long-term and large-scale behavior of the magnetic field at the solar surface is described rather well by the random-walk dispersal of a signed scalar, subject to the large-scale flows of meridional advection and differential rotation (*e.g.*, Sheeley *et al.*, 1983; Sheeley, Nash,

C.J. Schrijver (✉)
Dept. ADBS, Lockheed Martin Advanced Technology Center, Bldg. 252, 3251 Hanover St., Palo Alto, CA 94304-1191, USA
e-mail: schrijver@lmsal.com

Y. Liu
W.W. Hansen Experimental Physics Laboratory, Stanford University, Stanford, CA 94305-4085, USA
e-mail: yliu@sun.stanford.edu

and Wang, 1987; Wang, Nash, and Sheeley, 1989; Sheeley, 1992; Schrijver, 2001). Early on, this conclusion was based on simulations of large-scale patterns of the solar field that inject flux onto the photosphere by characterizing their position, size, orientation, and time of appearance. More recently, full-disk magnetogram sequences have been ingested into the flux-dispersal model (*e.g.*, Schrijver and DeRosa, 2003); this work also supports the general validity of the surface flux-dispersal concept.

Numerical experiments spanning more than a full solar cycle reveal some inconsistencies, however. For example, the cycle-to-cycle variation of the integrated sunspot number would be expected to cause substantial variations in the behavior of the field over the polar caps from one cycle to the next. In fact, some of these variations are so large that a purely two-dimensional flux-transport model predicts that some cycles should not see a polar-field reversal. This includes the reversal around 2000, which observations clearly showed to occur. This "hysteresis problem" can be avoided either by introducing a flux decay into the simulation that has an associated flux half-life time of order five to ten years (Schrijver, DeRosa, and Title, 2002), or by modulating the magnitude of the meridional advection by a factor of close to two from the weakest to the strongest sunspot cycle (Wang, Sheeley, and Lean, 2002).

The concept of flux decay reflects that the flux transport is not 2D, but fully 3D. Baumann, Schmitt, and Schüssler (2006) argue that the flux decay on the five to ten year time scale is a natural consequence of the turbulent diffusion of the magnetic field within the solar convection zone, in line with the interpretation proposed by Schrijver, DeRosa, and Title (2002). Observations of meridional flux transport over the past decade suggest that the meridional flow may in fact be variable on long time scales, although no definite information is available on such variations beyond the latest sunspot cycle. As there is evidence supporting both of the proposed solutions to the problem of long-term polar-field hysteresis associated with cycle-to-cycle variations, further research into their relative roles is warranted.

The availability of a full cycle of nearly continuous observations of the Sun's magnetic field, and frequent helioseismic measurements of the large-scale flow profiles at and below the surface, opens up the possibility of testing simulations against observables. Here, we study the behavior of the solar axial dipole moment over an 11-year period *i*) as measured from a series of SOHO/MDI (Scherrer *et al.*, 1995) synoptic maps (in Section 2), *ii*) as inferred from a flux-dispersal model based on magnetogram assimilation (Section 3), and *iii*) from a pure simulation model in which we can vary parameters to obtain a good match to the observations (Section 4).

This combination of observations and models is based on a single instrument, the Michelson Doppler Imager on SOHO, thus avoiding inter-instrument calibration problems. Moreover, the assimilation and pure simulation models have been tested against the MDI calibration in earlier studies (Schrijver, DeRosa, and Title, 2002; Schrijver and DeRosa, 2003), which have also yielded an initial flux distribution for the simulation and assimilation runs to start from in 1997 that is consistent with observations (as described in those studies).

The measurement of the global axial dipole moment of the Sun suffers from the problem that the polar fields are difficult to observe and properly calibrate, and that they are visible for only half of each year. We decided to assess the magnitude of this potential problem by looking at two metrics: one measuring the axial dipole moment for all flux equatorward of 75° in latitude (which avoids the partially visible polar caps and the regions very near the solar limb), and the axial dipole moment for all flux poleward of 60° (which is the edge of the flux-assimilation window in the assimilation model, beyond which the model fully determines the flux transport). We find that these two metrics yield consistent conclusions throughout our study.

2. MDI Synoptic Maps

A metric that can readily characterize the large-scale field of the Sun is the axial dipole moment, defined as an integral over the normalized surface area, thus equivalent to the solid angle Ω:

$$D = \frac{3}{4\pi} \int B_{\rm r} \sin(\theta)\, {\rm d}\Omega, \tag{1}$$

for radial flux density ($B_{\rm r}$) and heliographic latitude (θ). This quantity can be computed, for example, from a series of SOHO/MDI synoptic maps. In our case, we use the standard product for that with the revised calibration (Hoeksema *et al.*, 2008; Liu, Hoeksema, and Scherrer, 2008). Recently, MDI magnetograms have been recalibrated by correcting for the zero offset (Liu, Zhao, and Hoeksema, 2004) and the flux-density underestimate by applying a rescaling factor suggested by Tran *et al.* (2005).

For these synoptic maps, we use up to 20 pixels from 20 magnetograms to obtain the value for that pixel. In order to retain uniform effective integration time for every pixel, we allow a 60° selection window for remapped magnetograms within which a pixel could be selected. In this way, we can have a fairly uniform noise level over the synoptic maps (Hoeksema *et al.*, 2008).

The polar field for each chart was interpolated by using the observed data taken at the time when the Sun's north pole is tilting toward or away from SOHO. For each year, we take south polar-field data from a synoptic chart in March, and north polar-field data from a chart in September. Those data are then fitted by a two-dimensional polynomial function. The fitted data form a time-series polar-field data cube. The polar field for a chart is then interpolated from this data cube. The time when the 180° longitude passes the central meridian is used for this interpolation. To avoid unreliable observation near the limb, we replace the data in areas poleward of 75° by the results from the interpolation.

An area of concern for this study is, of course, the difficulty in measuring the high-latitude fields, both because the true polar regions can be observed for only part of each year, and because measurements of magnetic flux close to the solar limbs is notoriously difficult and subject to effects that include reduced resolution and the upward shift of the line formation region when going increasingly close to the limb. To isolate the potential problems for dipole moments that include the high-latitude field measurements, we compute and discuss the axial dipole moment $D_{<75}$ for the field between $\pm 75°$ in solar latitude as well as $D_{>60}$ for the field poleward of $\pm 60°$ in solar latitude, which is beyond the edge of the assimilation window discussed in Section 3.

Figure 1 shows the decrease of $D^{\rm syn}_{<75}$ and $D^{\rm syn}_{>60}$ based on the synoptic maps (dotted lines) with time, both crossing zero in early 2000, then growing again with the opposite sign. The values then reach a plateau by mid-2001, followed by what appears to be a moderate decrease. They end at about one-third and half of the absolute value for the beginning of the 11-year period, respectively. The most recent sunspot cycle thus presents us with the interesting fact that the axial dipole-moment reversal occurred about a year before cycle maximum (*cf.*, Figure 1), and that the ending magnitude is roughly half of the beginning value.

3. Assimilation Results

We can also compute axial dipole moments based on the assimilation model described in detail by Schrijver and DeRosa (2003). Their code continues to run without modification

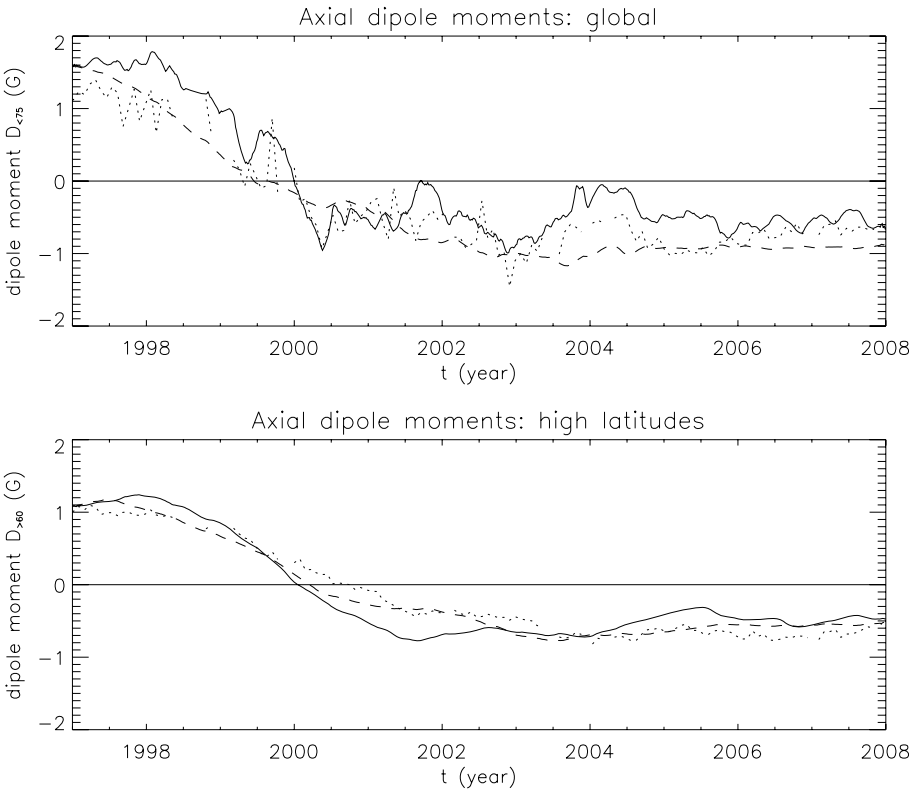

Figure 1 Top: Solar axial dipole moment $D_{<75}$ for fields below 75° in latitude through an 11-year sunspot cycle. Shown are values for $D_{<75}$ determined from SOHO/MDI synoptic maps (dotted), from our magnetogram assimilation model (solid), and from model run 10 (see Table 1; dashed). Bottom: Solar axial dipole moment $D_{>60}$ for fields above 60° in latitude through an 11-year sunspot cycle. Line styles as in the top panel.

since their original study. The axial dipole moments from the assimilation run are shown by the solid lines in Figure 1.

The total axial dipole moment for all latitudes for the initial condition of the assimilation model is 1.7 G. In view of the uncertainties of polar-field measurements, this compares well with the characteristic solar value at cycle minimum (see, for example, Wang and Sheeley, 2003).

The dipole moments based on the synoptic maps and on the assimilation runs compare reasonably well. The differences are caused by the different treatment of the latitudes poleward of 60°, differences in zero-point corrections, and different temporal resolutions (the assimilation run yields true synoptic maps updated on a six hour cadence, while what we generally refer to as "synoptic maps" are in fact diachronic maps pieced together from information near the central meridian). The differences between the two observation-based curves of a few tenths of a Gauss do not reveal significant systematic differences, and the timings of the sign change of the axial dipole moments differ by less than half a year for $D_{>60}$ and by much less that for $D_{<75}$.

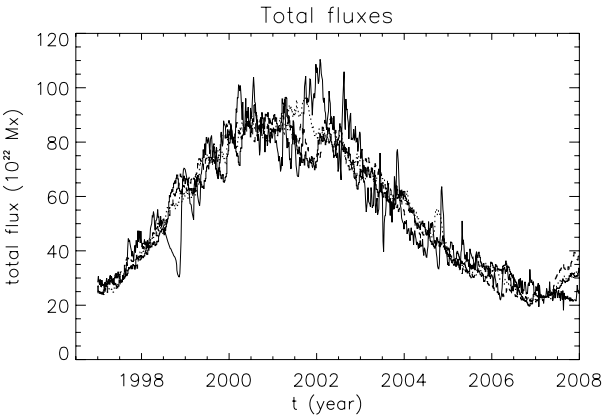

Figure 2 Total absolute flux in the various runs. The dark, solid curve is for the assimilation run 1. The solid, dotted, and dashed gray curves are for runs 2, 3, and 4 of the "standard" model, respectively (see Table 1). Note the artifacts in 1998 and early 1999 in the observation-based curve associated with the temporary loss of contact with SOHO and a subsequent extended roll period that was not used in the assimilation.

The axial dipole moment $D^{\rm syn}_{<75}$ associated with flux below 75° latitude by the end of 2008 decreases to −54% of its initial value at the start of 1997 based on the SOHO/MDI synoptic maps, while the value $D^{\rm syn}_{>60}$ for flux above 60° decreases to −56%. The corresponding values for $D^{\rm assim}_{<75}$ and $D^{\rm assim}_{>60}$ for the assimilation code are −37% and −56%.

4. Model Simulations

4.1. Standard Model Runs

We also use the pure simulation model as described by Schrijver, DeRosa, and Title (2002), including their best-fit value of five years for the half-life associated with the flux decay term described in Section 1. The only minor change that we have made is to remove the mild preferential orientation for ephemeral regions so that their orientation is completely random, consistent with recent observational results (Hagenaar, Schrijver, and Title, 2003).

We adjusted the amplitude of the cycle profile that determines the rate of "emergence" of active regions into the model so that the resulting total absolute flux in the model matches that of the assimilation run (see Figure 2). Apart from the delayed onset of the next cycle, anticipated for 2007, the total-flux profiles approximate the observations quite well.

Figure 3 compares the axial dipole moments based on the assimilation model with three runs of the simulation model (runs 2, 3, and 4 in Table 1). The latter three runs are identical in all respects, except that they were initialized from different random-number seed values. The differences are caused both by all of the random processes involved, primarily the active-region fluxes, positions, and tilt-angle orientations.

The "standard" model simulation runs end with axial dipole moments $D^{\rm sim}_{<75}$ and $D^{\rm sim}_{>60}$ that are −1.6 G and −1.0 G, respectively. The relative standard deviation in the mean $[\sigma/\sqrt{(N)}]$ for the $N = 3$ runs 2, 3, and 4, for the axial dipole moment at the end of the 11-year period is 20% for $D^{\rm sim}_{<75}$ and 10% for $D^{\rm sim}_{>60}$. This puts the solar observational results $7-10\,\sigma$ away from the standard model results.

There are no indications that the basic properties of solar active regions were any different in the latest sunspot cycle than in the earlier cycles whose properties were used to define the parent distribution functions for flux, latitude, and orientation used in the model runs. We note that the differential-rotation profile does not significantly affect the axial dipole moments (not at all in the linear approximation of the model; see the discussion by Schrijver and Zwaan (2000) and references therein, and the parameter study by Baumann *et al.*

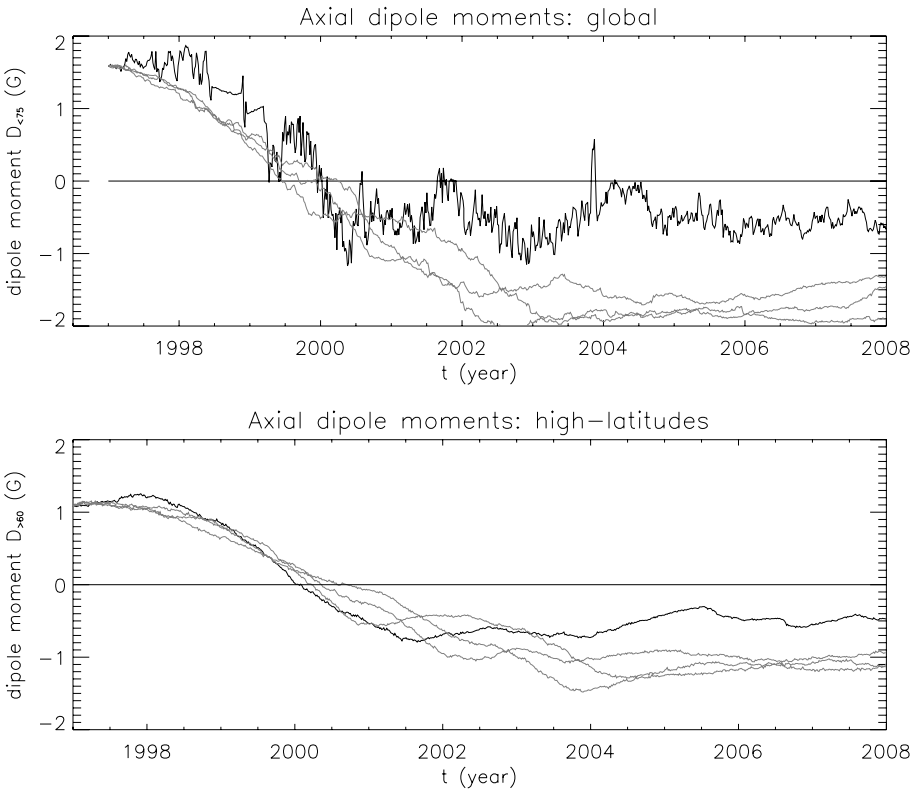

Figure 3 Top: Axial dipole moment $D_{<75}$ for flux below 75° in latitude from assimilation run 0 (black), and for "standard" model runs 2, 3, and 4 (gray; cf. Table 1). Bottom: As the top panel, but showing $D_{>60}$ for flux poleward of 60°.

(2004)). The meridional flow has a very strong effect, which we explore in detail in the next subsection.

Before we focus on the meridional advection, let us look at another important contributor to the global axial dipole moment, namely the tilt angle (γ) of the active region's dipole axis relative to the Equator. We looked at a sample of active regions to test whether $\langle\gamma\rangle$ for the latest cycle differs from earlier measurements. Starting from the NOAA Active Region lists, we select all active regions that were identified as on the solar disk for over seven consecutive days, while more than 30° away from any other active region throughout that period. For the purpose of this study we select only regions around the maximum of the solar cycle, covering the years 2000 through 2004. The resulting list contains 136 distinct active regions (their distribution in time and latitude is shown in the bottom panel of Figure 4).

For each of these active regions, we determine the center of gravity, weighting with the observed flux density for each pixel, for the two polarities separately. This is repeated for the first full-disk SOHO/MDI magnetogram past midnight on each successive day that the region is listed in the NOAA tables. The direction of the tilt angle of the region's dipole axis connecting the two centers of gravity is then determined and corrected for projection and B-angle effects.

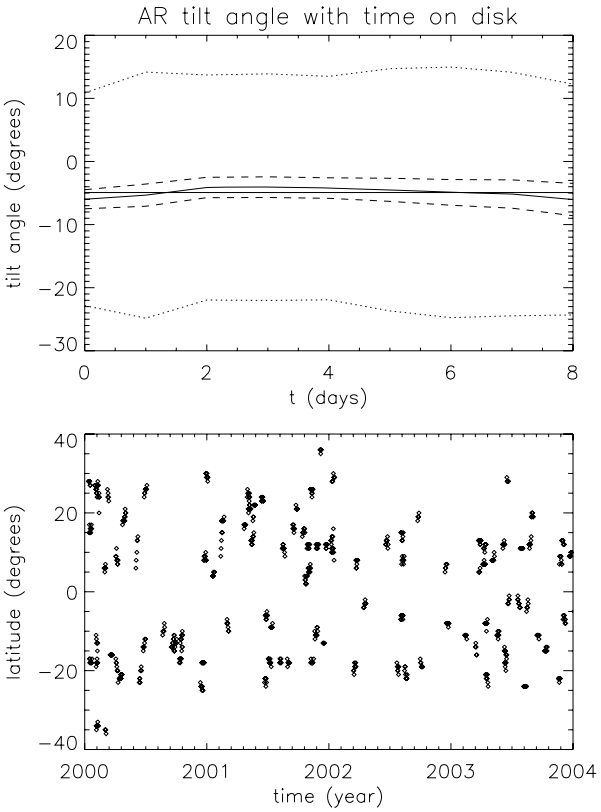

Figure 4 Top: Average active region tilt angles as a function of time on the disk; negative values signify tilts towards the Equator in both hemispheres. The dashed lines show the standard deviation in the mean; the dotted lines show the standard deviations of the sample. The grey horizontal line shows the average tilt angle of $-4.9°$. Bottom: Times and latitudes of the regions for which tilt angles were measured.

The average tilt angle as a function of the time that the active regions are visible on the solar disk is shown in Figure 4. The mean tilt angle is $\langle\gamma\rangle = 4.9° \pm 0.5°$ towards the Equator. This result is compatible at the 1.4σ level with the findings of Howard (1991) who found a mean value of $4.2° \pm 0.2°$. Figure 4 suggests that the observed tilt angle depends somewhat on the distance from central meridian: for regions midway their stay on the solar disk, and thus statistically nearer the central meridian, the observed tilt angle is very close to the value measured by Howard. Thus, it is likely that the instrumental resolution and projection effects on the solar surface for regions near the limb are responsible for raising the apparent value of $\langle\gamma\rangle$ somewhat over the true angle.

For the purpose of the present study, we point out that apart from a slight bias apparently related to projection effects away from disk center, there is no systematic change in the mean tilt angle over a period of up to eight days on the solar disk: the mean tilt angle with which the region emerges, is (close to) the mean tilt angle for the flux that disperses into the surrounding network (even though some regions will show preferred, sustained rotation of their tilt angles that may last for a few days).

4.2. Varying the Meridional Flow

The increased helioseismic coverage of the Sun by SOHO/MDI and GONG has enabled detailed studies of the strength and profile of the meridional flow, both near the surface and at some depth. The results of the analysis of these different data sets using either helioseismic

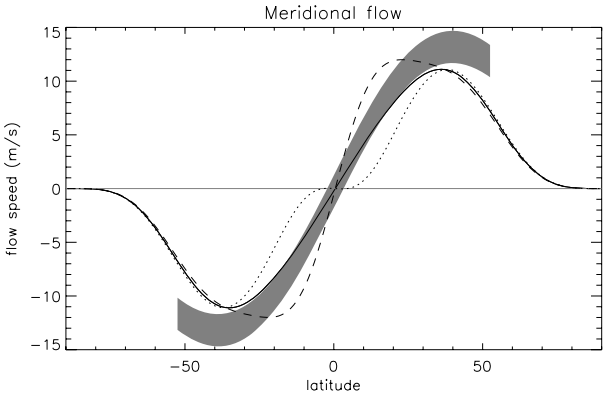

Figure 5 Examples of meridional-flow profiles used in the model runs. Solid: assimilation run 0; dotted: run 6; dashed: best-fit model run 10 (see Table 1). The shaded band shows a sample measured meridional flow profile based on correlation tracking, from Komm, Howard, and Harvey (1993), with an estimated uncertainty of 1.5 m s^{-1}.

methods (such as the time-distance technique) or correlation tracking on magnetic butterfly diagrams are in reasonable, but not perfect, agreement. For example, Švanda, Zhao, and Kosovichev (2007) compare time – distance and correlation – tracking results for Carrington rotation 1974 (in 2001) and they show that the two can differ by up to 5 m s^{-1} over latitude ranges of 10 – 20°, which is almost half of the 10 m s^{-1} that characterizes the flow speed poleward of ≈ 5° up to the end of the analyzed range at 40°.

It appears, however, that the intrinsic variations in the meridional-flow speed at depths from 3 – 9 Mm exceed these uncertainties: Švanda, Kosovichev, and Zhao (2007) (see also Zhao and Kosovichev, 2004), for example, use time-distance helioseismology for seven Carrington rotations from 1996 through 2006, and they see a marked change from year to year. The net effects of these changes over multiple years is a weakening of the meridional-flow speed at mid latitude by almost a factor of two around the middle of that period, associated with a slight steepening of the flows for the near-equatorial flows by a few meters per second up to 10° in latitude. Later in the period, the meridional flow appears to recover to its 1996 levels.

Švanda, Kosovichev, and Zhao (2007) point out that the weakening of the mid-latitude meridional flow during the cycle maximum phase is associated with a "countercell" of an outflow from the mean flux-emergence latitudes both towards the Equator and the poles, superimposed on the meridional flow. Although this shows up in the helioseismic results, they point out that these do not appear to influence the flux transport at the surface. In fact, they argue that "using the longitudinally averaged meridional flow profile from helioseismology in the solar cycle models for description of the flux transport is not justified." This perspective is shared by Gizon (2004) who finds that the localized flows with magnitudes up to 50 m s^{-1} cause variations of up to ≈ 5 m s^{-1} on the longitudinally-averaged flows determined from helioseismic inversions, which do not show up if the active regions and their immediate surroundings are masked out in the longitudinal averaging.

The studies quoted above suggest that the (near-)surface meridional flow that is associated with the surface flux transport appears to vary with time much less than the helioseismically determined flows at depth or around active regions. Measurements of the meridional flow at or close to the surface (as shown by, *e.g.*, Švanda, Kosovichev, and Zhao, 2007; González Hernández *et al.*, 2006) yield peak flow speeds of ≈ 10 m s^{-1} around latitudes of 20 – 40°. In view of this, we experiment with the flow profile used in earlier simulations, peaking at 10 m s^{-1} around 35° in latitude (*cf.*, Figure 5). We introduce a modification to that profile essentially limited to latitudes below 35° as follows.

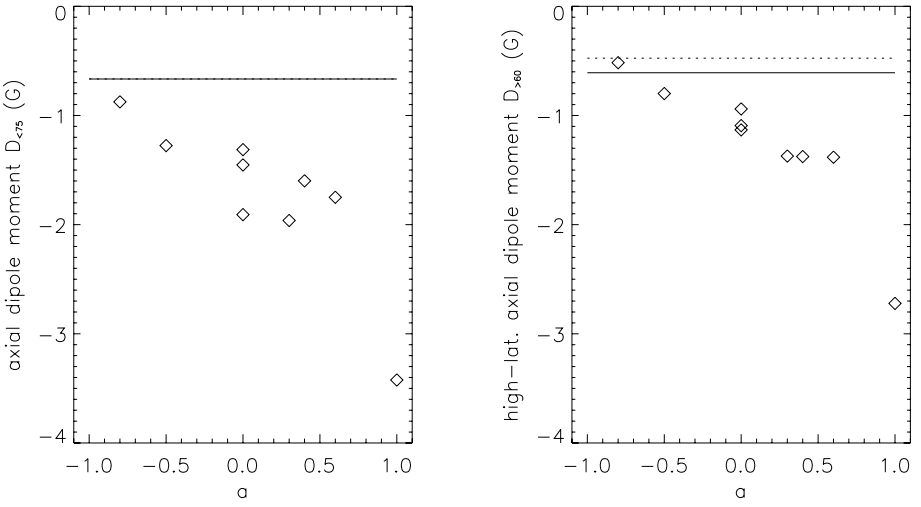

Figure 6 Left: Comparison of axial dipole moments $D_{<75}$ (G) for flux equatorward of 75° in latitude for the model runs listed in Table 1 (diamonds). The observed values from the assimilation run 0 and from the MDI synoptic maps for the end of 2007 are shown by solid and dotted lines, respectively (overlapping in this panel). Right: As on the left, but for $D_{>60}$ for flux poleward of 60°.

Starting from the parameterization used by Schrijver (2001), we introduce a modifying function $[g(\theta)]$, dependent on latitude (θ), in the meridional flow (v_{M}) across the model's solar surface:

$$v_{\mathrm{M}} = 15\big[\sin(2\theta)\, f\big(\theta'\big) f\big(\pi - \theta'\big) + g(\theta)\big] \tag{2}$$

($\mathrm{m\,s^{-1}}$), with a tapering function $f(\theta') = 1 - \exp(-(1.45\theta')^3)$, dependent on colatitude (θ', in radians), that is effective only poleward of a latitude of $\approx 40°$. This meridional flow resembles that used by Van Ballegooijen, Cartledge, and Priest (1998) who let the flow go to zero at $\approx 75°$ in order to model polar-crown filaments. Here, we add a function to modify the near-equatorial flow profile:

$$g(\theta) = 4a \sin(0.9\theta) \exp\big(-9\theta^2\big); \tag{3}$$

the shape and constants of proportionality are chosen so that the function has little effect above about 40° (see Figure 5).

As we increase the gradient in the meridional flow near the solar Equator, the northern and southern hemispheres are increasingly isolated from each other for the dispersing flux concentrations. The consequence of this is that the leading and following polarities are increasingly swept to the same pole, and that therefore the axial dipole moment is weakened (as has been recognized in multiple earlier studies by Wang, Sheeley, and Schrijver; referenced in Section 1). This is quantitatively summarized in Figure 6: in order for the model results to be compatible with the observed axial dipole moments, the near-equatorial meridional flow has to be substantially strengthened, with a best-fit multiplier for the expression in Equation (3) of $a \approx -0.8$, as for model run 10 in Table 1. Figure 1 (dashed line) shows that model run 10 does indeed yield axial dipole moments $D_{<75}^{\mathrm{sim}=10}$ and $D_{>60}^{\mathrm{sim}=10}$ that agree quite well with the observed values over the sunspot cycle. Comparing the meridional-flow profiles of the studies referenced above in this section among themselves, or with earlier measurements based on correlation tracking studies (*e.g.*, Komm, Howard, and Harvey (1993),

Table 1 Model runs, specifying the parameter a as in Equation (3)

Model	a	Comment
1	N/A	Standard assimilation model
2, 3, 4	0	Revised simulation model (see Section 4)
5	+1.0	Flow reversal near Equator
6	+0.6	No-flow zone at Equator
7	+0.4	
8	+0.3	
9	−0.5	
10	−0.8	Strongest flow from Equator

see Figure 5), shows that the modification of the flow profile introduced by $a = -0.8$ for Equation (3), is within the observational uncertainties (which include any variations of the flow profile over time).

5. Discussion and Conclusions

In this study, we combine synoptic maps, assimilation results, and model runs to study the evolution of the Sun's axial dipole moment during the recently completed sunspot cycle 23.

We find that the absolute value of the axial dipole moment in the most recent minimum for latitudes below 75° is $45 \pm 12\%$ lower than in the corresponding phase in early 1997.[1] This lies seven to ten standard deviations away from the value anticipated from numerical experiments based on observed solar properties in earlier cycles.

In a surface-flux transport model, the polar-field strength at times around cycle minima is a function of the strength and profile of the meridional advection. In the absence of meridional flow, for example, only random-walk diffusion carries some flux to the poles, but the long time that this takes allows for strong cancellation between flux from the dispersing active regions. As the flow strength increases, reduced cross-equatorial cancellation of the trailing relative to the leading polarities first leads to an increase of the polar-field strength, but a further increase begins to separate the two hemispheres, causing the polar-field strength to decrease again. The extensive parameter study by Baumann *et al.* (2004) shows that the strength peaks for a flow profile with a maximum around 8 m s^{-1} (dependent on the detailed profile, of course), *i.e.*, below the observed values. Hence, here we limit our numerical experiment leading to an increased separation of the northern and southern hemispheres by strengthening the meridional flow,[2] (*e.g.*, Wang, Sheeley, and Lean, 2002), particularly near

[1] Shortly after submission of this study, Sheeley (2008) reported that the number of polar faculae is also about half of that of the preceding cycle minimum, and in fact at their lowest value for an entire century.

[2] Note that Dikpati, de Toma, and Gilman (2008) have argued that a slowdown in meridional-flow speed leads to a weaker polar flux – contrary to what flux-dispersal models show, at least for the observed values of the surface meridional advection (see text). Their finding holds for a dynamo concept in which the meridional circulation spans the entire convection zone, and is in fact instrumental both in surface flux transport and in the internal field behavior. Hence, their finding on the relationship between meridional flow and polar-field strength is of a fundamentally different nature than that discussed by, *e.g.*, Sheeley, Wang, and DeVore (1989) or Wang, Sheeley, and Lean (2002; and references therein) which is limited strictly to the surface transport properties.

the Equator (alternatives are a reduction in the flux dispersal coefficient, or a reduced input strength of the axial dipole component (for example by a reduced mean tilt angle of the active regions relative to the Equator, for which we find no evidence, however).

We find that a modified meridional-flow profile, with an increased near-equatorial gradient, to peak at about 10 m s^{-1} around $15-20^{\circ}$ yields agreement between the observed, assimilated, and modeled large-scale axial dipole moments throughout a sunspot cycle to within the uncertainties associated with observational problems (poor polar visibility, zero-point corrections, and calibration issues) and statistical fluctuations (on fluxes and tilt angles of active regions).

Such a relatively rapid increase of meridional-flow speed with latitude is consistent with some observations (*e.g.*, Švanda, Kosovichev, and Zhao, 2007), but seems too rapid for other (*e.g.*, González Hernández *et al.*, 2006, who find the peak flow speed above $20-30^{\circ}$).

Hence, we could conclude that a modification of the meridional-flow profile that counters trans-equatorial flux transport can account for the weakened axial dipole moment at the end of 2007 compared to that at the start of 1997. That cannot be the whole story, however, for the years or decades prior to 1997, because making that same change to the meridional-flow profile for earlier cycles would result in a weakened polar-cap field and associated axial dipole moment in 1997. The strength of our initial-field configuration is, however, consistent with solar and heliospheric observations (see Schrijver, DeRosa, and Title, 2002).

Let us explore the consequences of the one free parameter in our model, namely the half life associated with flux decay, which was set to five years based on earlier studies (see references in Section 1). Rather than run a series of demanding simulations, we can learn what we need from a simple approximation to the problem at hand that allows an analytical solution. Let

$$x(t) = \cos(\omega t) \tag{4}$$

represent an oscillatory "dynamo action" that feeds axial dipole moment into the system, which changes the proxy for total axial dipole moment $y(t)$ in proportion to the "dynamo" input $x(t)$, with an exponential decay term for $y(t)$ with time constant β as follows:

$$\dot{y}(t) = \alpha\, x(t) - \beta y(t). \tag{5}$$

The general solution well beyond initialization of the system is

$$y(t) = \frac{\alpha}{(\omega^2 + \beta^2)^{1/2}} \sin(\omega t + \phi), \tag{6}$$

with the phase angle (ϕ) given by

$$\tan(\phi) = \frac{\beta}{\omega}. \tag{7}$$

For the simulations discussed above, $\beta = \ln(2)/5 = 0.14$ y^{-1}, so that with $\omega = 2\pi/22 = 0.29$ y^{-1}, $\phi = 26^{\circ}$, *i.e.*, $y(t)$ and $x(t)$ are somewhat out of the antiphase they would be in for $\beta = 0$. Although this very simple model ignores, *e.g.*, the asymmetry in sunspot-cycle profiles and the delays associated with the global flux dispersal from the emergence latitudes, we note that the change in axial dipole moment occurred about a year prior to cycle maximum (see Section 2) in the latest sunspot cycle, *i.e.*, with a phase difference equivalent to approximately 16°. With the very approximate model in Equation (7) such a phase difference requires a flux half-life of eight years, which lies within the range of five to ten years suggested in the study by Schrijver and DeRosa (2003). We point the interested

reader to a more general discussion of the analogous phase difference between sunspot cycle and solar open flux by Mackay, Priest, and Lockwood (2002) and by Schüssler and Baumann (2007), but do not pursue that issue further here.

If the change in meridional-flow effects on the axial dipole effectively modifies α to $\alpha_{\rm m} = \alpha/2$, then leaving the amplitude of $y(t)$ unchanged so that the initial value for 1997 can be maintained, would require $\beta_{\rm m}^2 = (\beta^2 - \omega^2)/2$. This cannot be achieved for a real value of $\beta_{\rm m}$ because $\omega > \beta$. In other words, no other choice of the flux decay time constant β could have yielded the initial axial dipole moment for 1997 if we were to apply the modified meridional flow for all cycles prior to 1997 (as in the simulations by Schrijver, DeRosa, and Title, 2002). Moreover, any such change in β would leave the 2008 values of the axial dipole moments too strong, unless β changed with time. Consequently, we conclude that at least the meridional-flow profile changed between one or more previous cycles and the most recent cycle.

We conclude that our study of the global axial dipole moment over the most recent sunspot cycle supports the general validity of the surface flux transport concept. It also lends strong support to the conclusion that the processes governing the global flux transport are subject to cycle-to-cycle changes. Comparison of our flux-transport model to assimilation and observational results yields no evidence that these changes are related to changes in the flux-input spectrum or, for example, in the active-region tilt angles. A modification of the differential flow profile that lies within the current observational uncertainties of order 5 $\mathrm{m\,s^{-1}}$ could be responsible.

Acknowledgements This work was supported by NASA grant NNG05GK33G of the LWS/TR&T program, and benefited from discussions with colleagues at SAIC in San Diego, California, and at the International Space Studies Institute (ISSI) in Bern, Switzerland. We thank the referee for helpful comments to improve the discussion of our results, and for references to related work in the literature, in particular regarding the non-monotonic consequences of the meridional flow.

References

Baumann, I., Schmitt, D., Schüssler, M.: 2006, *Astron. Astrophys.* **446**, 307.
Baumann, I., Schmitt, D., Schüssler, M., Solanki, S.K.: 2004, *Astron. Astrophys.* **426**, 1075.
Dikpati, M., de Toma, G., Gilman, P.A.: 2008, *Astrophys. J.* **675**, 920.
Gizon, L.: 2004, *Solar Phys.* **224**, 217.
González Hernández, I., Komm, R., Hill, F., Howe, R., Corbard, T., Haber, D.A.: 2006, *Astrophys. J.* **638**, 576.
Hagenaar, H.J., Schrijver, C.J., Title, A.M.: 2003, *Astrophys. J.* **584**, 1107.
Hoeksema, J.T., Liu, Y., Zhao, X.P., Amezcua, A.: 2008, in preparation.
Howard, R.F.: 1991, *Solar Phys.* **136**, 251.
Komm, R.W., Howard, R.F., Harvey, J.W.: 1993, *Solar Phys.* **147**, 207.
Liu, Y., Zhao, X., Hoeksema, J.T.: 2004, *Solar Phys.* **219**, 39.
Liu, Y., Hoeksema, J.T., Scherrer, P.H.: 2008, *Solar Phys.* in preparation.
Mackay, D.H., Priest, E.R., Lockwood, M.: 2002, *Solar Phys.* **209**, 287.
Scherrer, P.H., Bogart, R.S., Bush, R.I., Hoeksema, J.T., Kosovichev, A.G., Schou, J., Rosenberg, W., Springer, L., Tarbell, T.D., Title, A., Wolfson, C.J., Zayer, I., The MDI Engineering Team: 1995, *Solar Phys.* **162**, 129.
Schrijver, C.J.: 2001, *Astrophys. J.* **547**, 475.
Schrijver, C.J., DeRosa, M.L.: 2003, *Solar Phys.* **212**, 165.
Schrijver, C.J., Zwaan, C.: 2000, *Solar and Stellar Magnetic Activity*, Cambridge University Press, Cambridge.
Schrijver, C.J., DeRosa, M.L., Title, A.M.: 2002, *Astrophys. J.* **577**, 1006.
Schüssler, M., Baumann, I.: 2007, *Astron. Astrophys.* **459**, 945.
Sheeley, N.R.: 1992, In: Harvey, K.L. (ed.) *The Solar Cycle* **CS-27**, Astron. Soc. Pac., San Francisco, 1.
Sheeley, N.R., Nash, A.G., Wang, Y.M.: 1987, *Astrophys. J.* **319**, 481.

Sheeley, N.R., Wang, Y.M., DeVore, C.R.: 1989, *Solar Phys.* **124**, 1.
Sheeley, N.R., Boris, J.P., Young, T.R., DeVore, C.R., Harvey, K.L.: 1983, In: Stenflo, J.O. (ed.) *Solar and Stellar Magnetic Fields: Origins and Coronal Effects*, *IAU Symp.* **102**, Reidel, Dordrecht, 273.
Sheeley, N.R. Jr.: 2008, *Astrophys. J.* **680**, 1553.
Švanda, M., Kosovichev, A.G., Zhao, J.: 2007, *Astrophys. J. L* **670**, 69.
Švanda, M., Zhao, J., Kosovichev, A.G.: 2007, *Solar Phys.* **241**, 27.
Tran, T., Bertello, L., Ulrich, R.K., Evans, S.: 2005, *Astrophys. J. SS* **156**, 295.
Van Ballegooijen, A.A., Cartledge, N.P., Priest, E.R.: 1998, *Astrophys. J.* **501**, 866.
Wang, Y.M., Sheeley, N.R.: 2003, *Astrophys. J.* **591**, 1248.
Wang, Y.M., Nash, A.G., Sheeley, N.R.: 1989, *Astrophys. J.* **347**, 529.
Wang, Y.M., Sheeley, N.R., Lean, J.: 2002, *Astrophys. J.* **580**, 1188.
Zhao, J., Kosovichev, A.G.: 2004, *Astrophys. J.* **603**, 776.